The Astrophysical Journal, 813:48 (11pp), 2015 November 1 doi:10.1088/0004-637X/813/1/48

A GROUND-BASED ALBEDO UPPER LIMIT FOR HD 189733b FROM POLARIMETRY

Sloane J. Wiktorowicz[1,2], Larissa A. Nofi[3,1], Daniel Jontof-Hutter[4,5], Pushkar Kopparla[6], Gregory P. Laughlin[1], Ninos Hermis[1], Yuk L. Yung[6], and Mark R. Swain[7]
[1] Department of Astronomy and Astrophysics, University of California, Santa Cruz, CA 95064, USA; sloane.j.wiktorowicz@aero.org
[2] Remote Sensing Department, The Aerospace Corporation, El Segundo, CA 90245, USA
[3] Institute for Astronomy, University of Hawaii, Honolulu, HI 96822, USA
[4] Department of Astronomy, Davey Laboratory, Pennsylvania State University, University Park, PA 16802, USA
[5] NASA Ames Research Center, Moffett Field, CA 94035, USA
[6] Division of Geological and Planetary Sciences, California Institute of Technology, Pasadena, CA 91125, USA
[7] Jet Propulsion Laboratory, California Institute of Technology, 4800 Oak Grove Drive, Pasadena, CA 91109, USA
Received 2015 July 13; accepted 2015 September 29; published 2015 October 27

ABSTRACT

We present 50 nights of polarimetric observations of HD 189733 in the *B* band using the POLISH2 aperture-integrated polarimeter at the Lick Observatory Shane 3-m telescope. This instrument, commissioned in 2011, is designed to search for Rayleigh scattering from short-period exoplanets due to the polarized nature of scattered light. Since these planets are spatially unresolvable from their host stars, the relative contribution of the planet-to-total system polarization is expected to vary with an amplitude of the order of 10 parts per million (ppm) over the course of the orbit. Non-zero and also variable at the 10 ppm level, the inherent polarization of the Lick 3-m telescope limits the accuracy of our measurements and currently inhibits conclusive detection of scattered light from this exoplanet. However, the amplitude of observed variability conservatively sets a 99.7% confidence upper limit to the planet-induced polarization of the system of 60 ppm in the *B* band, which is consistent with a previous upper limit from the POLISH instrument at the Palomar Observatory 5-m telescope. A physically motivated Rayleigh scattering model, which includes the depolarizing effects of multiple scattering, is used to conservatively set a 99.7% confidence upper limit to the geometric albedo of HD 189733b of $A_g < 0.40$. This value is consistent with the value $A_g = 0.226 \pm 0.091$ derived from occultation observations with *Hubble Space Telescope* STIS, but it is inconsistent with the large $A_g = 0.61 \pm 0.12$ albedo reported by Berdyugina et al.

Key words: dust, extinction – planetary systems – planets and satellites: atmospheres – planets and satellites: individual (HD 189733b) – polarization – techniques: polarimetric

1. INTRODUCTION

Since the polarization of incident starlight scattered by a planetary atmosphere depends on the morphology, size, index of refraction, and vertical distribution of the scattering particles, scattered light polarimetry of planets presents a rich opportunity for the study of their atmospheres. In the Solar System, polarimetry has provided fascinating results for both Venus and Titan. For Venus, the significant negative branch polarization (i.e., with polarization vector oriented parallel to the Sun-Venus-observer "scattering plane"), and the peculiar variation of polarization as a function of phase angle (Lyot 1929; Coffeen & Gehrels 1969), are consistent with spherical, $1.05 \pm 0.10\,\mu$m radius cloud particles composed of a concentrated sulfuric acid solution (Hansen & Hovenier 1974). In contrast, Rayleigh scattering imparts positive branch polarization where polarization is oriented perpendicular to the scattering plane.

For Titan, large photochemical haze particles are suggested by the intensity in forward scattering (Rages et al. 1983), but small particles are implied by Titan's strong polarization ($P \sim 50\%$) at $\sim 90^\circ$ scattering angles from Pioneer 11 (Tomasko & Smith 1982) and *Voyager 1* and *2* observations (West et al. 1983). West (1991) suggested fractal aggregates for the shape of the aerosols, and West & Smith (1991) showed that such particles could reconcile the measurements of high polarization and strong forward scattering. Thus, the combination of polarimetry and photometry enabled the discovery that Titan's large, fractal haze particles are composed of thousands of small, spherical monomers (Tomasko & Smith 1982; West et al. 1983; Tomasko et al. 2009). Unfortunately, since polarimetry is most powerful when studying scattering through a large range in phase angles, the utility of ground-based polarimetry for most Solar System objects is limited. However, such a limitation is not present for most exoplanets, because time-variable phase angle $\alpha(t)$ is given by $\cos[\alpha(t)] = \sin i \cos[2\pi(t/T - 0.5)]$ for orbital inclination i and period T on a circular orbit (where $t = 0$ indicates mid-transit or inferior conjunction of the planet). Given the expectation value for randomly distributed orbital inclinations, $i_{\rm exp} \sim 52^\circ$, most exoplanets will traverse between $38^\circ < \alpha < 142^\circ$. Therefore, short-period exoplanets not only quickly sweep through a large range in phase angles, pronouncing them as desirable targets for scattered light polarimetry, but they also maximize intercepted starlight.

The hot Jupiter HD 189733b is an intriguing target for this study because of its large radius and close orbit, which maximize relative photon counts, and the brightness of its host star, which maximizes absolute photon counts. Interestingly, while a haze of small, Rayleigh-scattering particles is interpreted to be present in the atmosphere from *Hubble Space Telescope* (*HST*) STIS, ACS, and WFC3 observations (Lecavelier Des Etangs et al. 2008; Pont et al. 2008; Sing et al. 2009, 2011; Gibson et al. 2012; Huitson et al. 2012; Pont et al. 2013), this interpretation may be supplanted by the inaccurate subtraction of unocculted starspots (McCullough et al. 2014). While starspots may induce symmetry breaking of the stellar limb polarization (Chandrasekhar 1946a, 1946b), this effect is modeled to be at the ppm level or below in linear polarimetry, because the cross-sectional area of a starspot

vanishes at the limb (Berdyugina et al. 2011). However, transiting exoplanets are expected to impart symmetry breaking polarization at ingress and egress at the 10 ppm level or below in broadband (Carciofi & Magalhães 2005; Kostogryz et al. 2011, 2015; Wiktorowicz & Laughlin 2014). Investigation of this effect is beyond the scope of this paper. As with Titan, the presence of haze particles in HD 189733b may best be tested with a combination of photometry and polarimetry.

Surrounding occultation, when the exoplanet's disk dives behind the limb of the host star, (Evans et al. 2013, hereafter E13) find a significant change in the brightness of the system with *HST STIS*, which is interpreted as scattered light from the planet. Indeed, a weighted mean of the inferred geometric albedos of the planet in the 390–435 nm and 435–480 nm channels suggests a *B*-band albedo of $A_g = 0.226 \pm 0.091$. However, variability in the *B*-band linear polarization of the system was reported with an amplitude of order 100 ppm, which suggests a geometric albedo of $A_g = 0.61 \pm 0.12$ (Berdyugina et al. 2008, 2011). Our original polarimetric investigation found a 99% confidence upper limit to the variability of the system of 79 ppm, but these observations were taken unfiltered in a broader and redder bandpass (Wiktorowicz 2009). In an updated analysis of the sensitivity of the measurement, taking into account instrumental modulation efficiency, we determine the bandpass of the Wiktorowicz (2009) investigation to be 320–633 nm with a central wavelength of 437 nm. Regardless, both photometric and polarimetric investigations have provided inconclusive evidence for Rayleigh scattering in the atmosphere of HD 189733b.

We seek to utilize our significantly expanded data set to constrain the polarimetric amplitude, and therefore the albedo of the Rayleigh scattering surface, for this exoplanet. We briefly discuss the POLISH2 polarimeter at the Lick Observatory Shane 3-m telescope in Section 2 and observations of the HD 189733 system in Section 3. In Section 4, we discuss our observations in the context of this nascent field as well as paths toward improvements in data quality. Finally, we present concluding remarks in Section 5.

2. METHODS

2.1. The POLISH2 Polarimeter

In this section, we briefly describe POLISH2 (POlarimeter at Lick for Inclination Studies of Hot jupiters 2), and we refer the reader to Wiktorowicz & Nofi (2015) for further inquiry. Rather than using a conventional half waveplate to convert incident polarization into an intensity modulation that may be measured by conventional imaging detectors, POLISH2 employs two photoelastic modulators (PEMs). The stress birefringent property of the fused silica PEMs preferentially retards the electric field component oriented $\pm 45^\circ$ from the stress axis. When coupled with a Wollaston prism, the PEMs impart a nearly sinusoidal intensity modulation on the photomultiplier tube detectors. The resonant frequencies of the PEMs are 40 and 50 kHz, which causes linear and circular polarization to modulate at linear combinations of these frequencies. After high speed digitization of the detector outputs, software demodulation simultaneously measures Stokes $q = Q/I$, $u = U/I$ (fractional linear polarization), and $v = V/I$ (fractional circular polarization), which describe the fractional polarization of incident light.

The SNR of each measured Stokes parameter is proportional to the modulation efficiency of the PEMs. For example, a modulation efficiency of 100% imparts the theoretical maximum amplitude of photometric modulation onto the detectors, while a modulation efficiency of 50% reduces the amplitude of modulation to half this value. Mueller matrix modeling of POLISH2 shows that the modulation efficiencies of Stokes q, u, and v are 86%, 81%, and 56%, respectively. Therefore, it is expected that uncertainties in circular polarization measurements will be ~50% larger than in linear polarization.

While spatially resolved circular polarization of Jupiter has been detected at the ~100 ppm level from multiple scattering (Kemp & Swedlund 1971; Kemp & Wolstencroft 1971; Michalsky & Stokes 1974), the sign of circular polarization is observed to reverse between northern and southern hemispheres. For exoplanets, it is expected that the dilution of circular polarization by direct light from the host star, as well as from integrating over the planetary disk, will cause exoplanet circular polarization to be more difficult to measure than linear polarization.

The two major improvements in the use of PEMs over waveplates are as follows: (1) simultaneous Stokes q and u measurements obviate systematic effects from waveplate rotation (heterogeneity in retardance across the optic itself), from atmospheric or astrophysical changes on short timescales, and potentially doubles the throughput of the measurement; and (2) high speed modulation enables photon-limited sensitivity via $1/\sqrt{n_{\rm modulations}}$, where "modulation" is defined by sequential measurement of Stokes $\pm q$, for example. In contrast to PEMs, with a modulation timescale of order 10 μs, typical waveplate modulations have a duration of order minutes to minimize overhead due to waveplate rotation.

2.2. Observations and Calibration

To directly detect scattered light from spatially unresolvable exoplanets, the ability to measure nightly changes in the polarization of starlight at the 10 ppm level or below is required. In this regime, accuracy (the ability to calibrate non-astrophysical change to some level) is far more important than sensitivity (the ability to measure a change to that level). While photon noise defines the fundamental limit to the accuracy of a measurement, instrumental and atmospheric systematic effects tend to dominate for many exoplanet investigations. Therefore, it is crucial that these systematic effects be removed or calibrated to the 1 ppm level to enable confident detection of scattered light from exoplanets at the 10 ppm level. We identify and partially correct for two dominant systematics: polarized sky foreground and non-zero telescope polarization.

As the POLISH2 field of view is ~15″ in diameter, a detectable quantity of sky photons is present even in the *B* band. This foreground tends to be polarized, especially when the moon lies ~90° from the target. To mitigate this systematic effect, we perform one 30-s integration on a sky field 30″ N of the target for every two integrations on-target. Therefore, one-third of all telescope time is devoted to monitoring sky polarization with a cadence of one minute.

At the focus of a telescope, detectable polarization is measured even when observing an unpolarized star. This is because reflectivity variations across the telescope mirrors cause a discrepancy in the intensities of pairs of light rays with equal but opposite incidence angles, which causes the

polarization from certain patches of the mirror to dominate. Even at Cassegrain focus of a variety of telescopes, this so-called "telescope polarization" is found by many authors to be 10–100 ppm in amplitude (Hough et al. 2006; Wiktorowicz & Matthews 2008; Lucas et al. 2009; Wiktorowicz 2009; Berdyugina et al. 2011; Wiktorowicz & Nofi 2015).

The standard approach for measuring telescope polarization is to observe a handful of nearly unpolarized calibrator stars. In practice, however, the details of this process may impart additional systematics that may be misinterpreted as arising from the science target. For instance, Lucas et al. (2009) observe that 12 of their 75 telescope polarization measurements are inconsistent with the mean value of telescope polarization at the $>3\sigma$ level, and they consequently reject these measurements. However, the probability of this occurrence in a normally distributed population is $\sim 10^{-9}$. Lucas et al. (2009) therefore note that the measurements must have a non-Gaussian distribution and advocate for repeated measurements if possible. We concur with this request, and we also caution that rejecting calibrator measurements that lie $>3\sigma$ from the mean will introduce a bias into the science results, because measurements may not be drawn from a Gaussian distribution.

In addition, we advocate that the observing cadence on calibrator stars follow that of the science targets, lest biases be introduced. Wiktorowicz (2009) observes the same calibrator star during each night in the study, but the use of only one calibrator limits the accuracy of the zero point of polarization measurements. However, accurate measurement of the time-averaged polarization of an exoplanet host star is necessary only to describe the state of the intervening ISM dust particles and has no relevance to the scattering properties of an exoplanet atmosphere. Wiktorowicz (2009) found the square root of the weighted variance of nightly telescope polarization observations to be $\sigma_q = 7.5$ ppm and $\sigma_u = 5.3$ ppm (Wiktorowicz 2009, Table 4), while the upper limit to exoplanet variation was found to be 79 ppm. Therefore, observation of calibrator and science targets with the same nightly cadence enabled calibrations to be an order of magnitude more accurate than science observations. Observing the same five calibrator stars nearly every night, Lucas et al. (2009) expand this approach to accurately measure telescope polarization each night. While Berdyugina et al. (2011) observe 26 calibrator stars over 15 nights, the dates of observation for each star are not presented. Indeed, the long duration of each calibrator star observation, one to two hours, implies that very few calibrators were observed on successive nights. In an investigation where systematic effects are severe, it is imperative that the same control and science targets be observed during each night.

Therefore, we observe 3 to 12 telescope polarization calibrator stars during each night of a given run, and the nightly target list is reproduced for each night of the run. Depending on the time of year, the makeup of this list will of course vary based on observability. These stars are identified from both the PlanetPol group (Hough et al. 2006; Lucas et al. 2009; Bailey et al. 2010) and our own unpublished survey of nearby, bright stars with POLISH2 at the Lick Observatory Nickel 1-m telescope. Given that interstellar polarization scales roughly linearly with heliocentric distance (e.g., Hall 1949; Hiltner 1949; Fosalba et al. 2002), nearly unpolarized stars are expected to lie in the vicinity of the Sun. Due to this proximity, such suitable stars tend to be quite bright. Therefore, sufficient measurement sensitivity is typically obtained after nine minutes for each telescope polarization calibrator star.

Strongly polarized stars ($p = \sqrt{q^2 + u^2} \sim 1\%$) represent the second type of calibrator. These stars are typically observed to determine the rotational position of the instrument; that is, the relationship between instrumental Stokes (q', u') and celestial (q, u). We typically observe the same two strongly polarized stars for nine minutes during each night of a run. Wiktorowicz & Nofi (2015) discuss absolute calibration of POLISH2 via sequential, laboratory injection of 100% Stokes q, u, and v. POLISH2 has recently demonstrated the ability to measure linear polarimetric variations at the 10^{-5} level over a single, 3.8-hr observation on an object only two magnitudes brighter than HD 189733. Spatial inhomogeneity in the surface albedo of asteroid (4) Vesta causes rotational modulation in its disk-integrated linear polarization. The amplitude of modulation varies with Sun-asteroid-observer phase angle, and POLISH2 has measured a peak-to-peak value of 294 $\pm$ 35 ppm (Wiktorowicz & Nofi 2015). Given the comparable amplitudes of polarization variations between (4) Vesta and HD 189733, as well as the comparable quantity of photons detected per period ($\propto 10^{-0.4\,m} \times T$ for apparent magnitude m and period T), these observations show that POLISH2 is uniquely positioned to measure the polarimetric variability of spatially unresolvable exoplanet systems.

3. RESULTS

We performed 50 nights of B-band observations of HD 189733 with POLISH2 at the Lick 3-m telescope between 2011 August 13 and 2014 July 14 UT. Observing duration typically varied from one to three hours per night, depending on the time of year and weather. Table 1 lists the stars observed during this program, where previous estimates of the degree of linear polarization are shown in the last column. Nightly mean telescope polarization is listed in Table 2, where $n_{\rm star}$ denotes the number of nearly unpolarized calibrator stars observed each night. MJD values are only tabulated to one decimal place because many of these stars are typically observed throughout the night. Table 3 presents nightly measurements of the linear and circular fractional polarization (Stokes q, u, and v) of the HD 189733 system subtracted by telescope polarization. Degree of linear polarization $p \approx \sqrt{q^2 + u^2}$ (but see note below) and position angle of linear polarization $\Theta = \frac{1}{2}\arctan(u/q)$. Uncertainties in the last two digits of each entry are denoted by the quantities in parentheses. For values of p consistent with zero, Θ is undefined and is therefore given by ellipses. The uncertainty in MJD values describe half of the duration of each nightly measurement. These values are binned in orbital phase in Table 4, and they are subtracted by the time-averaged polarization listed in the first line of that table. As discussed in Section 2.1, the modulation efficiency for circular polarization is significantly lower than that for linear polarization. Thus, the uncertainties in Stokes v measurements are expected to be larger than those for Stokes q and u.

Since the magnitude of a vector is biased in the presence of noise, we employ the generalized MAS estimator (Plaszczynski et al. 2014) to estimate the degree of linear polarization p. Briefly, this estimator corrects the naive calculation $p = \sqrt{q^2 + u^2}$, which is positive definite, to account for measurement uncertainties in q and u. Such correction is especially important for measurements with SNR ≈ 1, and it is

Table 1
Observed Stars

Star Name	HD	HR	R.A. (J2000)	decl. (J2000)	d (pc)	B	Spec. Type	p (ppm)	References
HD 189733	189733		20 00 43.7	+22 42 39.06	19.5	8.58	K0V+M4V	300.7(6.4)	1
α And	358	15	00 08 23.3	+29 05 25.55	29.7	1.95	B8IV-VHgMn	100(1200)	2
α Ari	12929	617	02 07 10.4	+23 27 44.70	20.2	3.17	K1IIIb	300(1200)	2
β Tri	13161	622	02 09 32.6	+34 59 14.27	38.9	3.14	A5III	500(1200)	2
ν Tau	25490	1251	04 03 09.4	+05 59 21.48	35.9	3.94	A0.5Va	400(1200)	2
π^3 Ori	30652	1543	04 49 50.4	+06 57 40.59	8.1	3.63	F6V	400(1200)	2
38 Lyn	80081	3690	09 18 50.6	+36 48 09.33	38.3	3.88	A1V	500(1200)	2
θ UMa	82328	3775	09 32 51.4	+51 40 38.28	13.5	3.64	F7V	100(1200)	2
β Leo	102647	4534	11 49 03.6	+14 34 19.41	11.0	2.22	A3Va	2.3(1.1)	3
β Vir	102870	4540	11 50 41.7	+01 45 52.99	10.9	4.15	F9V	3.3(1.4)	3
η Boo	121370	5235	13 54 41.1	+18 23 51.79	11.4	3.25	G0IV	3.5(1.8)	3
α Boo	124897	5340	14 15 39.7	+19 10 56.67	11.3	1.18	K0III	6.3(1.6)	3
γ Boo	127762	5435	14 32 04.7	+38 18 29.70	26.6	3.21	A7III	3.6(1.6)	3
ζ Her	150680	6212	16 41 17.2	+31 36 09.79	10.7	3.43	G0IV	9.6(2.6)	3
η Her	150997	6220	16 42 53.8	+38 55 20.11	33.3	4.42	G7.5IIIb	1300(1200)	2
ζ Aql	177724	7235	19 05 24.6	+13 51 48.52	25.5	3.00	A0IV-Vnn	22.8(3.0)	3
ι Cyg	184006	7420	19 29 42.4	+51 43 47.21	37.2	3.92	A5V	–	–
α Aql	187642	7557	19 50 47.0	+08 52 05.96	5.1	0.98	A7Vn	7.4(1.3)	3
ϵ Cyg	197989	7949	20 46 12.7	+33 58 12.93	22.3	3.52	K0III-IV	50(200)	2
θ Peg	210418	8450	22 10 12.0	+06 11 52.31	28.3	3.62	A1Va	500(1200)	2
α Lac	213558	8585	22 31 17.5	+50 16 56.97	31.5	3.78	A1V	400(200)	2

References. (1) Wiktorowicz (2009), (2) Heiles (2000), (3) Bailey et al. (2010).

found to be more accurate than Rician (Rice 1945) or Wardle–Kronberg corrections (Wardle & Kronberg 1974). Given that our analysis utilizes repeated measurements binned in orbital phase, and that nightly measurements tend to lie at low SNR, such correction is important.

3.1. Telescope Polarization

The 50 nights of HD 189733 observations were obtained over nine observing runs between 2011 August and 2014 July. An average of eight nearly unpolarized calibrator stars were observed during each of these runs for a total of 20 individual stars (Table 1). A total of 367 observations of such calibrator stars were performed, which represents a wealth of information on the B-band linear/circular polarization and stability of nearby stars. Indeed, high accuracy observations of nearby stars are essential in understanding the galactic magnetic field in the solar vicinity (Bailey et al. 2010; Frisch et al. 2010, 2012, 2015). We determine telescope polarization on a nightly basis from the weighted mean value of each Stokes parameter (Table 2). Figure 1 compares linear polarization of these stars in a q–u diagram, where measurements are subtracted by telescope polarization, while linear and circular polarization are compared in Figure 2. Both a histogram and the cumulative distribution function of values of p are shown in Figure 3. The square root of the weighted variances of all 367 observations are $\sigma_q = 22$, $\sigma_u = 12$, and $\sigma_v = 32$ ppm. We find that 75% of our B-band measurements have $p < 31$ ppm, while this value is 20 ppm for the optical red (590–1000 nm) observations of Bailey et al. (2010). Thus, our measurements are broadly consistent with PlanetPol observations of nearby stars (Bailey et al. 2010). We also present a large sample of B-band circular polarimetric observations of nearby stars, where 75% of measurements have $|v| < 47$ ppm (Figure 4). This is consistent with the smaller subset of observations published in Wiktorowicz & Nofi (2015).

3.2. HD 189733

Figure 5 shows nightly Lick 3-m/POLISH2 observations in the B band, while Figure 6 presents binned Stokes q, u, and p observations of the HD 189733 system, both from this study (Lick 3-m/POLISH2, B band) and from Wiktorowicz (2009; Palomar 5-m/POLISH, unfiltered). Both POLISH and POLISH2 measurements are subtracted by their time averages to highlight the time-variable component, and degree of linear polarization Δp is recalculated from Δq and Δu. Binned values of Δp are calculated from binned values of Δq and Δu. Also shown in Figure 6 are Rayleigh scattering models with geometric albedos of 0.231, 0.434, and 0.604. A detailed description of these models is given in Kopparla et al. (2015). In addition, we show the model fitting the reported detection from Berdyugina et al. (2011), which represents a geometric albedo of 0.61 ± 0.12 and is calculated using only single scattering. While it is clear that our model cannot be varied to explain our observations, the POLISH and POLISH2 data are intriguingly consistent. In particular, a high degree of linear polarization is observed near orbital phase 0.1, which is inconsistent with our Rayleigh scattering model. We note that while the data sets of Berdyugina et al. (2008; KVA 0.6-m/DIPol) and Berdyugina et al. (2011; NOT 2.5-m/TurPol) appear similar, and are also taken with different instrument and telescope combinations, this POLISH2 study dramatically improves the combination of telescope aperture and nights of observation on HD 189733.

On average, each bin is composed of repeated observations on five nights at the same orbital phase (Figure 6), and the bin uncertainty is given by either the square root of the weighted variance or the standard error of the measurements. This choice is determined by whether the measurements in each bin are inconsistent with each other at the 3σ level from a χ^2 test. This tests whether measurements in each bin are drawn from a normally distributed population, because standard error decreases as $1/\sqrt{n}$ only for normally distributed measurements.

Table 2
Nightly Telescope Polarization (TP) Observations

UT Date	MJD	n_{star}	q (ppm)	u (ppm)	p (ppm)	Θ (°)	v (ppm)
2011 Aug 13	55786.3	3	+111.3(4.8)	+98.3(4.1)	148.5(4.5)	20.73(85)	−14(10)
2011 Aug 14	55787.3	6	+102.0(2.7)	+84.6(2.3)	132.5(2.6)	19.85(54)	−46.0(6.0)
2011 Aug 15	55788.3	6	+94.1(2.7)	+80.1(2.3)	123.5(2.6)	20.21(58)	−6.9(6.0)
2011 Aug 16	55789.3	6	+106.0(2.9)	+99.8(2.5)	145.6(2.7)	21.63(52)	−21.0(6.3)
2011 Aug 17	55790.3	12	+103.4(2.8)	+89.3(2.4)	136.6(2.6)	20.40(53)	−61.7(6.0)
2012 May 05	56052.3	8	+6.5(2.9)	+50.3(2.5)	50.6(2.5)	41.3(1.7)	−22.1(6.5)
2012 May 06	56053.3	8	+11.2(3.1)	+59.7(2.6)	60.6(2.6)	39.7(1.4)	−19.6(6.7)
2012 May 07	56054.3	8	+11.6(3.0)	+59.5(2.6)	60.5(2.6)	39.5(1.4)	−11.6(6.6)
2012 May 08	56055.3	8	+8.0(2.8)	+57.9(2.4)	58.4(2.4)	41.1(1.4)	+17.5(6.2)
2012 May 09	56056.3	8	+5.2(2.8)	+55.0(2.4)	55.1(2.4)	42.3(1.5)	+5.7(6.1)
2012 Jun 07	56085.4	8	+29.6(2.9)	+71.1(2.5)	77.0(2.6)	33.7(1.1)	−39.9(6.5)
2012 Jun 08	56086.3	10	+40.9(2.8)	+71.7(2.4)	82.5(2.5)	30.14(94)	−33.0(6.2)
2012 Jun 09	56087.3	10	+30.6(3.0)	+70.7(2.6)	77.0(2.6)	33.3(1.1)	−22.3(6.6)
2012 Jun 10	56088.3	6	+94.3(3.7)	+85.1(3.2)	127.0(3.5)	21.03(77)	−33.3(8.1)
2012 Jun 11	56089.3	10	+27.0(2.8)	+66.3(2.4)	71.5(2.5)	33.9(1.1)	+21.9(6.2)
2012 Jun 12	56090.3	10	+45.3(2.9)	+71.0(2.5)	84.2(2.6)	28.72(95)	−34.7(6.4)
2013 May 24	56436.3	5	+41.5(6.0)	+67.2(5.1)	78.8(5.3)	29.2(2.1)	−51(13)
2013 May 25	56437.2	7	+86.8(4.8)	+99.0(4.1)	131.6(4.4)	24.38(98)	−42(10)
2013 May 26	56438.2	7	+37.0(4.7)	+72.2(4.0)	81.0(4.1)	31.4(1.6)	−74(10)
2013 May 27	56439.3	3	+76(10)	+87.3(8.5)	115.2(9.2)	24.5(2.3)	−80(22)
2013 May 29	56441.2	7	+65.4(6.2)	+85.7(5.3)	107.6(5.6)	26.3(1.6)	+62(14)
2013 May 30	56442.2	7	+75.7(4.8)	+83.9(4.1)	112.9(4.4)	24.0(1.1)	−68(10)
2013 May 31	56443.2	7	+54.1(4.5)	+71.5(3.9)	89.6(4.1)	26.4(1.4)	−52.0(9.9)
2013 Aug 17	56521.4	3	+66(17)	+83(14)	105(16)	25.8(4.4)	−45(37)
2013 Aug 18	56522.4	11	+113.5(3.9)	+114.9(3.4)	161.5(3.6)	22.67(65)	−66.2(8.6)
2013 Aug 19	56523.4	11	+81.3(4.2)	+110.6(3.6)	137.2(3.8)	26.83(84)	−24.6(9.3)
2013 Aug 20	56524.4	10	+128.6(4.7)	+140.2(4.0)	190.2(4.3)	23.74(66)	−48(10)
2013 Aug 21	56525.4	10	+90.9(4.2)	+101.9(3.7)	136.5(3.9)	24.13(84)	−17.5(9.3)
2013 Aug 22	56526.4	11	+68.4(4.0)	+101.5(3.5)	122.3(3.6)	28.02(90)	−17.1(8.9)
2013 Sep 11	56546.3	8	+63.8(4.2)	+55.8(3.6)	84.7(4.0)	20.6(1.3)	−62.9(9.4)
2013 Sep 12	56547.3	8	+63.3(4.3)	+64.4(3.7)	90.2(4.0)	22.7(1.3)	−55.6(9.6)
2013 Sep 13	56548.3	8	+68.6(4.2)	+57.1(3.6)	89.1(3.9)	19.9(1.2)	−44.4(9.2)
2013 Sep 14	56549.3	8	+63.2(4.1)	+70.5(3.6)	94.6(3.8)	24.1(1.2)	−39.6(9.2)
2013 Sep 15	56550.3	8	+61.3(4.1)	+62.4(3.5)	87.4(3.8)	22.7(1.2)	−49.4(9.1)
2013 Sep 16	56551.3	8	+62.0(4.0)	+51.9(3.4)	80.7(3.7)	20.0(1.3)	−13.8(8.7)
2013 Oct 11	56576.3	7	+50.0(4.3)	+51.9(3.7)	71.9(4.0)	23.1(1.6)	+134.9(9.5)
2013 Oct 12	56577.3	7	+45.3(4.2)	+56.4(3.6)	72.2(3.9)	25.6(1.6)	−148.4(9.4)
2013 Oct 13	56578.3	7	+60.3(4.5)	+48.6(3.9)	77.3(4.3)	19.4(1.5)	−212(10)
2013 Oct 14	56579.3	7	+47.0(4.0)	+61.3(3.4)	77.1(3.7)	26.2(1.4)	−53.6(8.9)
2014 Jun 07	56815.2	5	+63.8(3.1)	+62.1(2.7)	88.9(2.9)	22.11(94)	−31.4(6.9)
2014 Jun 08	56816.2	6	+90.8(2.0)	+85.3(1.7)	124.6(1.9)	21.60(43)	−1.7(4.5)
2014 Jun 09	56817.2	6	+85.3(2.0)	+82.6(1.7)	118.7(1.8)	22.04(44)	+58.9(4.4)
2014 Jun 10	56818.3	6	+78.0(1.9)	+81.4(1.7)	112.7(1.8)	23.11(46)	−2.5(4.3)
2014 Jun 11	56819.2	6	+86.8(2.0)	+84.9(1.7)	121.4(1.9)	22.18(44)	+20.2(4.5)
2014 Jun 12	56820.2	6	+74.9(1.9)	+85.6(1.6)	113.7(1.8)	24.41(45)	+18.4(4.2)
2014 Jun 13	56821.2	6	+68.3(1.9)	+81.6(1.7)	106.4(1.8)	25.03(50)	−40.7(4.3)
2014 Jul 10	56848.2	4	+50.8(1.9)	+87.2(1.6)	100.9(1.7)	29.89(52)	−43.1(4.2)
2014 Jul 11	56849.2	4	+54.9(1.9)	+85.0(1.6)	101.2(1.7)	28.56(50)	+16.5(4.1)
2014 Jul 12	56850.2	4	+51.6(1.8)	+83.5(1.6)	98.2(1.7)	29.14(52)	−10.3(4)
2014 Jul 13	56851.2	4	+49.7(1.9)	+85.5(1.7)	98.8(1.7)	29.92(54)	−24.9(4.3)
2014 Jul 14	56852.2	4	+48.4(1.9)	+87.7(1.6)	100.1(1.7)	30.55(52)	−37.0(4.2)
2014 Jul 15	56853.2	4	+31.1(9.8)	+79.4(8.4)	84.8(8.6)	34.3(3.3)	−25(22)

Indeed, it can be seen that the uncertainties near orbital phase 0.5 and 0.85 are large due to relative disagreement between successive observations at these orbital phases (Figure 5). Therefore, polarization accuracy is hampered by systematic effects arising from telescope polarization variations. While is it possible that the significant variations between bins in Figure 6 arise from complicated scattering mechanisms in the HD 189733 system, we conservatively assume that these are caused by the known presence of telescope systematic effects.

Even if all variations are solely caused by telescope polarization, the amplitude of the scatter in degree of polarization p is only ∼50 ppm (Figure 6). This is clearly an interesting accuracy regime, as the scattered light amplitude of HD 189733b has been measured to ∼100 ppm from *HST STIS* (E13) in total intensity. To determine an upper limit to the polarimetric amplitude due to the planet, and thereby constrain the albedo of the exoplanet, we perform bootstrap resampling of our measurements. For the binned Stokes q and u data sets in

Table 3
Nightly HD 189733 Observations, TP-subtracted

UT Date	MJD	q (ppm)	u (ppm)	p (ppm)	Θ (°)	v (ppm)
2011 Aug 13	55786.289(51)	+62(38)	+120(32)	131(33)	31.4(7.9)	−27(81)
2011 Aug 14	55787.286(54)	+34(31)	+35(27)	41(29)	23(20)	+69(68)
2011 Aug 15	55788.286(55)	+69(30)	+33(26)	72(30)	13(11)	+48(66)
2011 Aug 16	55789.287(55)	+46(31)	+55(27)	66(29)	25(13)	+40(69)
2011 Aug 17	55790.283(55)	+32(32)	+81(27)	82(28)	34(11)	+74(70)
2012 May 05	56052.455(37)	+98(33)	−63(29)	113(32)	163.5(7.6)	+149(73)
2012 May 06	56053.459(35)	+57(35)	−101(30)	110(32)	149.7(8.8)	−39(78)
2012 May 07	56054.448(41)	+18(30)	+74(26)	70(26)	38(12)	+136(67)
2012 May 08	56055.450(40)	+24(31)	−6(26)	16(30)	173(51)	−52(68)
2012 May 09	56056.446(42)	−59(29)	+14(25)	55(29)	83(13)	+104(65)
2012 Jun 07	56085.430(32)	+18(34)	+47(30)	40(30)	35(22)	+111(76)
2012 Jun 08	56086.432(30)	−5(36)	+102(31)	96(31)	46(10)	+52(79)
2012 Jun 09	56087.435(27)	−34(37)	−59(32)	59(33)	120(17)	−48(82)
2012 Jun 10	56088.456(17)	+10(47)	+42(41)	29(41)	38(43)	+60(100)
2012 Jun 11	56089.434(29)	+73(36)	+5(30)	67(36)	2(13)	+16(78)
2012 Jun 12	56090.436(28)	−42(36)	+76(31)	80(32)	60(12)	−54(79)
2013 May 24	56436.434(67)	+19(32)	+169(27)	166(27)	41.9(5.5)	+78(71)
2013 May 25	56437.428(71)	+15(31)	+138(26)	136(26)	41.9(6.4)	+51(67)
2013 May 26	56438.3569(91)	−56(81)	+85(70)	77(74)	62(27)	+140(180)
2013 May 27	56439.448(51)	−3(37)	+82(33)	73(33)	46(14)	+101(83)
2013 May 29	56441.410(58)	−40(46)	+87(39)	85(40)	57(15)	−71(100)
2013 May 30	56442.407(90)	−55(28)	+143(24)	150(25)	55.5(5.3)	−58(61)
2013 Aug 17	56521.307(73)	+48(40)	+87(35)	92(36)	31(12)	−70(90)
2013 Aug 18	56522.32(11)	−38(27)	+98(22)	102(23)	55.6(7.3)	−96(59)
2013 Aug 19	56523.34(10)	+22(29)	+60(25)	58(25)	35(14)	−23(63)
2013 Aug 20	56524.379(51)	+85(45)	+58(38)	95(43)	17(12)	−290(99)
2013 Aug 21	56525.31(11)	+107(27)	+43(23)	113(27)	11.0(6.0)	−236(61)
2013 Aug 22	56526.32(10)	+111(30)	+41(25)	116(29)	10.1(6.3)	−78(64)
2013 Sep 11	56546.29(10)	+18(26)	+45(22)	42(22)	34(16)	−55(56)
2013 Sep 12	56547.28(10)	−28(29)	+22(25)	28(27)	71(27)	−75(64)
2013 Sep 13	56548.279(99)	−51(25)	+74(22)	86(23)	62.3(8.0)	−63(57)
2013 Sep 14	56549.28(10)	−3(25)	+32(21)	24(21)	48(27)	−95(56)
2013 Sep 15	56550.275(99)	+58(24)	+47(21)	71(23)	19.7(9.0)	−75(54)
2013 Sep 16	56551.27(10)	+27(24)	+47(20)	49(21)	30(13)	−127(53)
2013 Oct 11	56576.237(95)	+8(26)	+2(23)	4(26)	⋯	−48(57)
2013 Oct 12	56577.228(80)	+68(28)	+46(25)	78(27)	16.9(9.6)	+166(65)
2013 Oct 13	56578.217(83)	−15(32)	+3(27)	9(32)	⋯	+68(69)
2013 Oct 14	56579.220(80)	−11(26)	+2(23)	7(26)	⋯	+15(58)
2014 Jun 07	56815.387(96)	+86(27)	+53(23)	98(26)	15.9(7.1)	−174(59)
2014 Jun 08	56816.386(96)	−7(26)	+20(22)	13(23)	54(52)	−41(57)
2014 Jun 09	56817.385(98)	+23(26)	+58(22)	58(22)	34(12)	+63(57)
2014 Jun 10	56818.392(91)	+44(27)	+26(23)	46(26)	15(15)	−15(60)
2014 Jun 11	56819.386(98)	+20(26)	−29(22)	28(23)	152(24)	−35(57)
2014 Jun 12	56820.387(97)	+15(25)	+22(21)	19(22)	28(34)	+39(55)
2014 Jun 13	56821.389(97)	−46(25)	+25(22)	47(24)	76(14)	−90(56)
2014 Jul 10	56848.35(14)	−20(21)	+11(18)	17(21)	76(32)	−19(47)
2014 Jul 11	56849.35(14)	+32(22)	+20(19)	33(21)	16(17)	−109(48)
2014 Jul 12	56850.35(14)	+26(21)	+16(18)	25(21)	16(22)	−59(48)
2014 Jul 13	56851.36(14)	+46(25)	+65(22)	76(23)	27.3(9.1)	−76(56)
2014 Jul 14	56852.36(14)	+44(22)	+27(19)	48(21)	16(12)	+60(49)

Figure 6, we perform 10^4 iterations of 10^4 resampled data sets with the following procedure: (1) the orbital phase value of each bin is randomly assigned from the list of 11 bins, (2) each observable quantity (Stokes q and u) is resampled from its nightly mean and uncertainty, and the uncertainty is retained, and (3) degree of polarization p is calculated for each bin from the generalized MAS estimator (Section 3).

Since bootstrap resampling randomly assigns an orbital phase value for each synthetic data point, but exoplanet polarization is strongly correlated with orbital phase, bootstrap resampling cannot directly test whether observational data are consistent with scattering models. Indeed, bootstrap resampling is an investigation into the noise properties of the observational data, and it allows the maximum polarization amplitude of those models to be constrained.

Measurement of a linear polarization vector requires two sets of observations in an orthogonal basis. Stokes q represents the fractional polarization component in the north-south ($+q$) and east-west ($-q$) directions in the plane of the sky, while Stokes u represents the component in the northeast–southwest ($+u$) and

Table 4
Binned HD 189733 Observations

Phase	q (ppm)	u (ppm)	p (ppm)	Θ (°)	v (ppm)
Time Avg.	+15.9(4.0)	+39.5(3.5)	42.4(3.6)	34.1(2.7)	−17.9(9.0)
0.061(21)	+17(15)	−42(13)	43(13)	145.8(9.7)	−21(33)
0.150(35)	−19(13)	+9(43)	12(22)	⋯	−7(28)
0.217(38)	−27(13)	+21(11)	32(12)	71(10)	+6(28)
0.313(29)	+15(14)	−6(12)	12(13)	169(28)	−44(30)
0.407(28)	−4(16)	−25(14)	21(14)	130(21)	+35(35)
0.504(31)	+13(11)	+17(49)	13(40)	⋯	+4(78)
0.614(23)	+1(16)	−13(14)	8(14)	136(49)	+69(35)
0.697(43)	−5(18)	+41(15)	38(15)	48(13)	−17(40)
0.758(26)	+8(14)	−13(12)	11(12)	151(32)	−15(31)
0.852(27)	−22(14)	−22(39)	22(29)	112(41)	+40(30)
0.958(34)	+13(11)	+8.1(9.2)	13(10)	16(21)	+5(24)

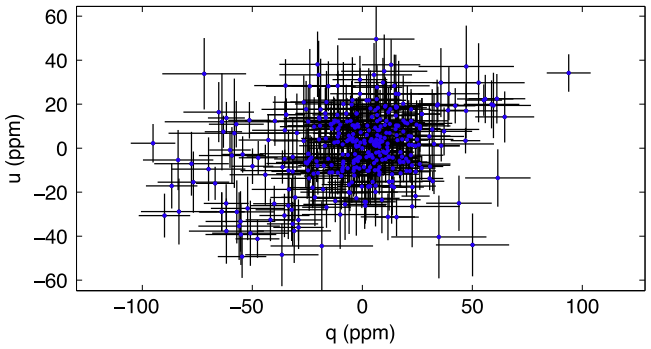

Figure 1. Fractional linear polarimetry of all nearly unpolarized calibrator stars.

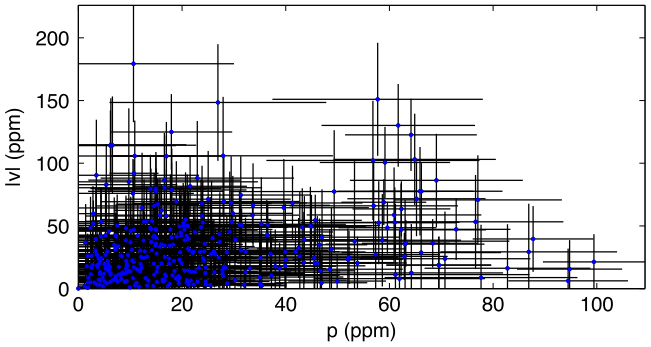

Figure 2. Fractional linear and circular polarimetry of all nearly unpolarized calibrator stars.

northwest–southeast ($-u$) directions. If the orientation of the exoplanet orbital plane seen by the observer were known a priori (the longitude of the ascending node of the system, Ω), the observer may simply rotate the telescope or instrument about the optical axis such that instrumental Stokes q' (i.e., "up" on the detector as opposed to the direction toward celestial north) were aligned with the orbital plane. In the case that any interstellar polarization, inherent polarization of the host star, and polarization from an exozodiacal disk were all zero, Stokes u' would then be constant and Stokes q' would equal the degree of linear polarization p'. However, since Ω is unknown, the astrophysically interesting quantity p must be calculated from

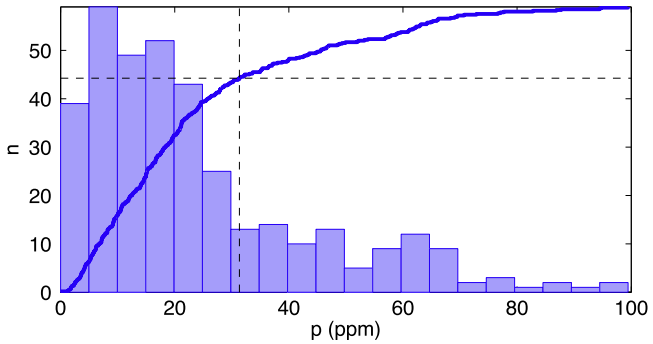

Figure 3. Histogram and cumulative distribution function of degree of linear polarization p measurements of nearly unpolarized calibrator stars. 75% of these measurements have $p < 31$ ppm (dashed lines).

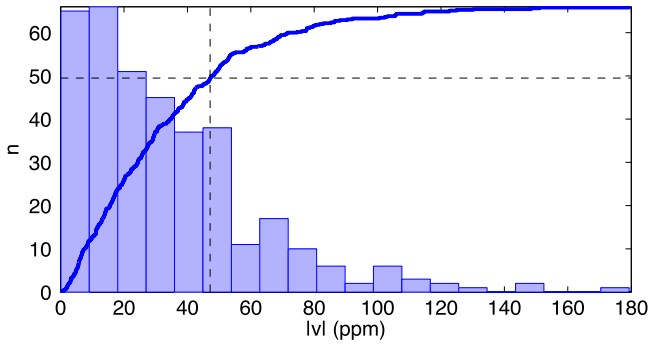

Figure 4. Histogram and cumulative distribution function of circular polarization (Stokes $|v|$) measurements of nearly unpolarized calibrator stars. 75% of these measurements have $p < 47$ ppm (dashed lines).

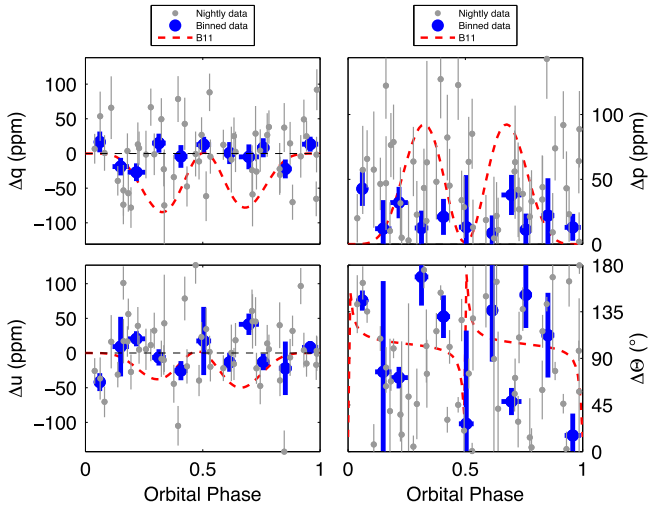

Figure 5. Nightly (gray points) and binned (blue points) B-band observations of HD 189733 vs. orbital phase from Lick 3-m/POLISH2, where phase 0 corresponds to mid-transit and 0.5 to occultation. The Berdyugina et al. (2011, hereafter B11) single scattering model is shown as red, dashed curves.

the variations in Stokes q and u in order to present a conclusive detection of scattered light from an exoplanet.

For this investigation, with a goal of albedo constraint as opposed to detection, we perform a χ^2 analysis between the values of p from bootstrap resampling and the modeled polarization phase curves. While it is possible to perform a bootstrap analysis on Stokes q and u data separately, the uncertain geometry of the system in the plane of the sky (Ω) introduces an additional free parameter that would significantly

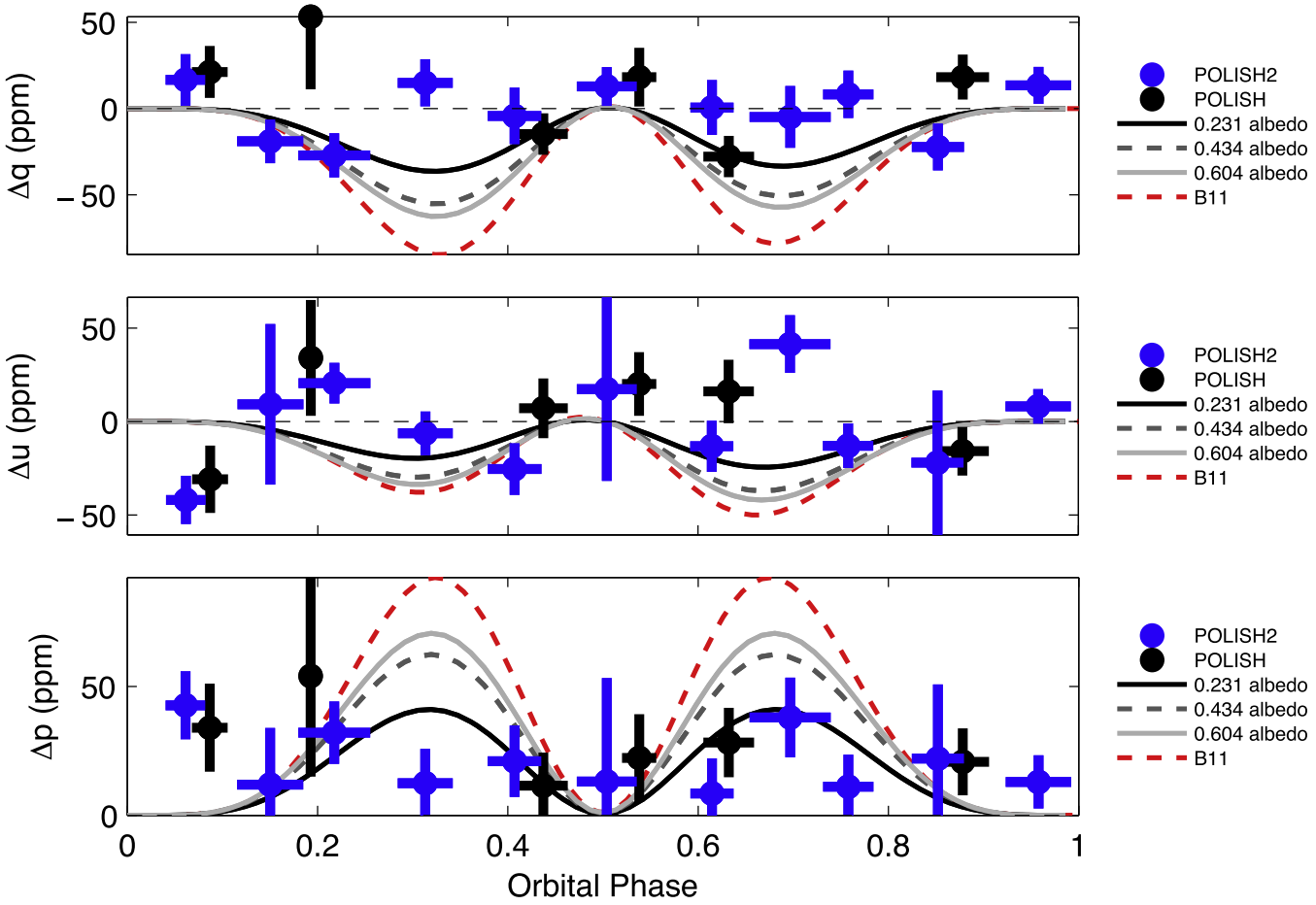

Figure 6. Phase-binned observations of HD 189733 vs. orbital phase. Lick 3-m/POLISH2 *B*-band data are shown in blue, and Palomar 5-m/POLISH unfiltered data are shown in black (Wiktorowicz 2009). An intriguing consistency exists between these data, which were taken with two different instruments on two different telescopes. Multiple scattering models with albedos 0.231, 0.434, and 0.604 are shown and compared to a single scattering model with albedo 0.61 (B11). All models use a longitude of the ascending node of $\Omega = 16°$ as from B11.

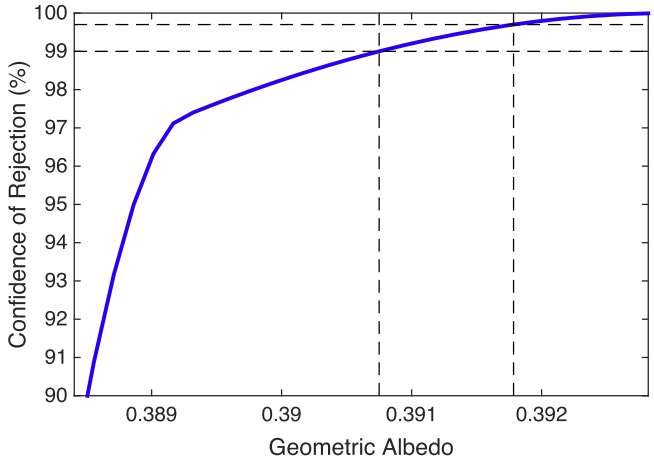

Figure 7. Results from a single iteration of 10^4 resampled datasets, where geometric albedos >0.39 may be rejected with 99.7% confidence (see dashed lines for 99.7% and 99% confidence upper limits). 9999 additional iterations cause this upper limit to converge to $A_g < 0.40$ (Figure 8).

complicate the analysis. In the extreme case, where $\Omega = 0°$, 45°, 90°, or 135°, no variations would be detected in one of Stokes q or u. One might then place an upper limit to the polarization of the planet that was erroneously low. Performing the bootstrap analysis on p obviates such concerns, because p is invariant through rotation ($p = p'$). However, care must be taken in this analysis because the purpose is to reject model *amplitudes* rather than the models themselves. This is because our observations appear to be limited by systematic effects and prohibit conclusive detection at this time.

Even with systematic effects present, however, large-amplitude polarization variations from the exoplanet may be rejected with confidence by synthetic data whose polarization values are lower than model values. This is because the χ^2 residuals between low polarization data and the models directly test whether high-amplitude variations would have been detectable. While synthetic data having polarization higher than the model values also generate large χ^2 residuals, these data clearly should not be able to reject high-amplitude polarization variations from the exoplanet. Thus, a simple χ^2 test between all synthetic data and models cannot be used to constrain the polarization amplitude due to the planet. Instead, since synthetic data with polarization higher than model values cannot constrain the amplitude of planet polarization, we remove the contribution of these data to the χ^2 residuals. Rather than simply deleting these data, which would reduce the degrees of freedom in the χ^2 test and bias the result toward lower polarization amplitudes, we set their χ^2 residuals to zero but retain their degrees of freedom. Thus, our bootstrap analysis provides a conservative upper limit to the polarization amplitude of the planet.

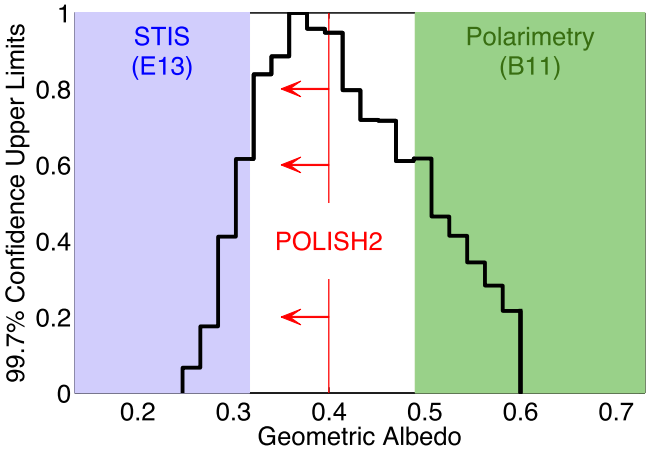

Figure 8. Histogram of 99.7% confidence upper limits to the HD 189733b geometric albedo from 10^4 iterations of χ^2 analyses between 10^4 bootstrap resampled datasets (resampled from Figure 6, bottom panel) and modeled phase curves (Kopparla et al. 2015). Note that a single iteration of 10^4 resampled datasets is shown in Figure 7. Geometric albedos larger than 0.40 may be rejected with 99.7% confidence (median of bootstrap histogram, red line). The 0.226 ± 0.091 albedo from *HST STIS* photometry (E13) cannot be excluded with our data, while the reported 0.61 ± 0.12 albedo from polarimetry (B11) may be rejected with >99.99% confidence.

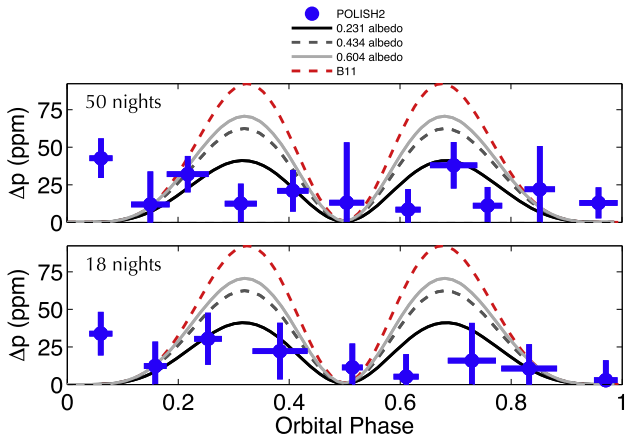

Figure 9. Comparison of degree of polarization from the full, 50-night dataset (2011 August–2014 July) with an 18-night subset (2013 September–2014 July).

The albedo constraint from a single bootstrap iteration out of 10^4, which itself contains 10^4 resampled data sets, is shown in Figure 7. Figure 8 shows the distribution of these χ^2 analyses, where Rayleigh scattering models with geometric albedos larger than 0.40 may be rejected by our observations with 99.7% confidence. By interpolating the amplitude of modeled degree of polarization versus geometric albedo, we find a 99.7% confidence upper limit to the linear polarimetric amplitude of HD 189733b to be 60 ppm in the *B* band. Table 4 shows that both the time averaged circular polarization, and any variability phase-locked to the orbital period of the planet, are consistent with zero.

4. DISCUSSION

Some POLISH2 measurements of HD 189733, repeated at the same orbital phase months or years later, differ at the 3σ level (i.e., orbital phase 0.5 and 0.85, Figures 5 and 6). This suggests that telescope systematic effects play a significant role in the accuracy of our observations. However, it is possible that the significant variations in Figure 6 are due in part to complicated scattering processes in the HD 189733 system, which appear to be supported by an intriguing similarity between POLISH and POLISH2 observations near orbital phase 0.1. However, further investigation of this effect is not justified by the current data set and is consequently beyond the scope of this manuscript. The most conservative assessment of the data set assigns all variations to uncorrected systematic effects arising from telescope polarization. From this assumption, bootstrap resampling provides a 99.7% confidence upper limit to the geometric albedo of HD 189733b of $A_g < 0.40$ in the *B* band. The *B*-band POLISH2 bandpass of 391–482 nm ($\lambda_c = 441$ nm) is essentially identical to the combined 390–435 nm and 435–480 nm channels of *STIS*. From *STIS* observations, a weighted mean of the albedo estimates from these channels (E13) suggests an HD 189733b albedo of 0.226 ± 0.091 in *B* band. Figure 8 shows that POLISH2 observations are currently unable to constrain the albedo of HD 189733b further than the study by Evans et al. (2013).

However, Figure 8 illustrates that even the 1σ lower bound to the reported 0.61 ± 0.12 albedo from previous polarimetry (Berdyugina et al. 2011) is ruled out by POLISH2 observations with over 99.99% confidence. Our current observations, comprising 50 nights of data spanning three years, present a 99.7% confidence upper limit to the polarimetric modulation of the exoplanet to be 60 ppm in the *B* band. Figure 9 shows a subset of our observations comprising 18 nights between 2013 September and 2014 July. The similarity between this and the full 50-night data set (Figure 6) suggest that accuracy does not continue to improve as $1/\sqrt{n_{\rm nights}}$, which is expected from measurements dominated by systematic effects with a non-Gaussian distribution. However, this also shows that high polarimetric accuracy may be obtained from the ground, on a modest telescope, and after a reasonable observing campaign. The observations of Wiktorowicz (2009), taken over six nights in a single run using a different telescope and instrument (Palomar 5-m/POLISH), provide an upper limit of 79 ppm with 99% confidence. We note that the wavelength range reported by Wiktorowicz (2009), roughly 400–675 nm, neglected a PEM modulation efficiency term; correction for this effect shifts the true bandpass to 320–633 nm ($\lambda_c = 437$ nm). Therefore, we confirm (and extend to *B* band) the conclusion of Wiktorowicz (2009) that the large, ~100 ppm polarimetric amplitude reported from previous polarimetry (Berdyugina et al. 2008, 2011) cannot be due to polarized, scattered light from the HD 189733b hot Jupiter.

Indeed, given the known radius of the exoplanet from transit photometry, a large, $A_g \approx 0.6$ albedo requires a model including single scattering only. This is because the inclusion of multiple scattering, expected in an atmosphere with high albedo, acts to randomize electric field orientations through successive scattering and thereby depolarize light scattered by the exoplanet atmosphere (Buenzli & Schmid 2009; Lucas et al. 2009; Kopparla et al. 2015). However, the long-standing observation of circular polarization in scattered light from the poles of Jupiter (Kemp & Swedlund 1971; Kemp & Wolstencroft 1971; Michalsky & Stokes 1974) requires the presence of multiple scattering. Thus, it is reasonable to expect that since multiple scattering is required to understand the

scattered light from Jupiter, with geometric albedo $A_g = 0.52$, models of scattered light from Jovian exoplanets must also include multiple scattering.

We suggest that hitherto unidentified systematic effects cause spurious polarization measurements with the polarimeters used in previously reported exoplanet polarimetry (Berdyugina et al. 2008, 2011). While PEM polarimeters such as PlanetPol and POLISH2 have demonstrated accuracies of order 10 ppm in the literature on inter- (Bailey et al. 2010) and intra-night timescales (Wiktorowicz & Nofi 2015), we suggest that the low modulation frequency and asynchronous observation of Stokes q and u inherent in waveplates may prevent exoplanet scattered light detections with waveplate polarimeters.

Our difficulty in the accurate correction for telescope polarization lies with the equatorial mount of the Lick 3-m telescope, because stellar and telescope polarization cannot be separated through observation at varying parallactic angle. This requires nightly observation of nearly unpolarized stars, whose weak polarization is a direct result of their proximity to Earth due to the linear dependence of interstellar polarization with heliocentric distance (e.g., Hall 1949; Hiltner 1949; Fosalba et al. 2002). Since these calibration stars are by definition nearby and bright, they are necessarily distributed nearly uniformly across the sky. Thus, it is possible that the varying gravitational environment of the telescope introduces a change to the telescope polarization between science and calibration targets. The addition of data at similar exoplanet orbital phases, but taken during different times of year, may include such a variable component of telescope polarization. However, self calibration of telescope polarization during observation of the science target has been shown to enable high accuracy for the Gemini Planet Imager (Wiktorowicz et al. 2014), which is mounted at the alt-az Gemini South 8-m telescope. With the telescope de-rotator powered down, instrumental and telescope polarization vectors do not rotate with parallactic angle in the instrument frame, while stellar polarization does. Therefore, it is expected that a POLISH2-like instrument mounted at an alt-az telescope of greater than 3-m aperture will provide the highest accuracy observations necessary to detect scattered light from close-in exoplanets. This represents the best of both worlds, utilizing the superior accuracy of PEMs over waveplates and the enhanced calibration environment of alt-az telescopes over equatorial ones.

However, even from a 60-year-old, equatorial 3-m telescope overlooking the tenth largest city in the United States, we have demonstrated accuracy sufficient to test specific exoplanet results from the space-based, 2.4-m *HST*. From our extensive observations of nearly unpolarized calibrator stars (Table 2), we plan to correlate telescope polarization with telescope altitude and azimuth to enable a flexure correction to Lick 3-m/POLISH2 observations. In addition, beginning with our 2014 June observations, we have altered our calibration strategy to bracket exoplanet observations with periodic observations of the same nearly unpolarized calibrator stars during each night. These observations will further improve the accuracy of flexure correction. Finally, rather than binning mean nightly data in orbital phase, we will re-bin data from run to run according to their 0.1 s data segments. This enables any variability on hourly timescales to be binned properly, which may reduce systematic effects and increase accuracy.

Even absent these improvements to calibration, POLISH2 accuracy is currently capable of detecting polarization of any close-in exoplanet with an amplitude larger than 60 ppm given sufficient observing time. While HD 189733b was observed due to its close-in orbit, large radius, and bright host star, other targets exist whose expected polarimetric amplitudes are larger than our systematic noise floor. We have already begun observations of such exoplanets.

While we have consistently asserted that telescope systematic effects are the likely cause of the deviation between our HD 189733 observations and a simple Rayleigh scattering model, it is known that some exoplanets harbor asymmetric features in scattered light (i.e., Demory et al. 2013) that may have polarized counterparts. It is possible that the high degree of polarization observed near orbital phases 0.1 and 0.7, as well as the low degree of polarization observed near orbital phase 0.3, may be manifestations of complicated scattering behavior in the HD 189733b exoplanet. We refer the reader to Kopparla et al. (2015) for theoretical discussion of such possibilities.

5. CONCLUSION

From 50 nights of HD 189733 observations with the POLISH2 polarimeter at the Lick 3-m telescope, we constrain the geometric albedo of HD 189733b to be $A_g < 0.40$ in the B band with 99.7% confidence. This value is consistent with the 0.226 ± 0.091 albedo from *STIS* photometry determined by Evans et al. (2013), but we reject the reported 0.61 ± 0.12 albedo from previous polarimetry with over 99.99% confidence (Berdyugina et al. 2011). The conclusive detection of Rayleigh scattering from this exoplanet is of the highest significance for exoplanet science, because HD 189733b has become the poster child for the recent finding of hazes on exoplanets (Lecavelier Des Etangs et al. 2008; Pont et al. 2008; Sing et al. 2009, 2011; Gibson et al. 2012; Huitson et al. 2012; Pont et al. 2013). However, photometric techniques potentially have a mundane explanation for tantalizing suggestions of Rayleigh scattering, as inaccurate subtraction of unocculted starspots may masquerade as a signature of Rayleigh scattering (McCullough et al. 2014). Given the requirement that high accuracy exoplanet science be repeatable, and given the predisposition to resort to space-based inquiry, we demonstrate the virtue of long temporal baseline, ground-based study of exoplanets using complementary techniques afforded by the physics of the photon.

While our observations appear to be limited by systematic effects at the 60 ppm level, which are inherent in equatorial telescopes, we are currently observing a sample of exoplanets expected to provide larger amplitudes in polarized light. We are also in the process of performing additional calibration measures, via empirical telescope flexure correction, that may reduce the systematic noise floor from the Lick 3-m telescope. Additionally, we have previously demonstrated the utility of self-calibration on science targets with polarimeters at large, alt-az telescopes (Wiktorowicz et al. 2014). Therefore, we advocate for POLISH2-like, photoelastic polarimeters at large, modern telescopes for the conclusive detection of scattered light from a large sample of close-in exoplanets.

We would like to acknowledge the tireless efforts of the Lick Observatory staff. This work was performed (in part) under contract with the California Institute of Technology (Caltech) funded by NASA through the Sagan Fellowship Program

executed by the NASA Exoplanet Science Institute. S.J.W. and L.A.N. acknowledge support from the NASA Origins of Solar Systems program through grant NNX13AF63G. P.K. and Y.L.Y. acknowledge support from an NAI Virtual Planetary Laboratory grant from the University of Washington to the Jet Propulsion Laboratory and California Institute of Technology. Research at Lick Observatory is partially supported by a generous gift from Google.

Facility: Shane (POLISH2).

REFERENCES

Bailey, J., Lucas, P. W., & Hough, J. H. 2010, MNRAS, 405, 2570
Berdyugina, S. V., Berdyugin, A. V., Fluri, D. M., & Piirola, V. 2008, ApJL, 673, L83
Berdyugina, S. V., Berdyugin, A. V., Fluri, D. M., & Piirola, V. 2011, ApJL, 728, L6 (B11)
Buenzli, E., & Schmid, H. M. 2009, A&A, 504, 259
Carciofi, A. C., & Magalhães, A. M. 2005, ApJ, 635, 570
Chandrasekhar, S. 1946a, ApJ, 103, 351
Chandrasekhar, S. 1946b, ApJ, 104, 110
Coffeen, D. L., & Gehrels, T. 1969, AJ, 74, 433
Demory, B.-O., de Wit, J., Lewis, N., et al. 2013, ApJL, 776, L25
Evans, T. M., Pont, F., Sing, D. K., et al. 2013, ApJL, 772, L16 (E13)
Fosalba, P., Lazarian, A., Prunet, S., & Tauber, J. A. 2002, ApJ, 564, 762
Frisch, P. C., Andersson, B.-G., Berdyugin, A., et al. 2010, ApJ, 724, 1473
Frisch, P. C., Andersson, B.-G., Berdyugin, A., et al. 2012, ApJ, 760, 106
Frisch, P. C., Andersson, B.-G., Berdyugin, A., et al. 2015, ApJ, 805, 60
Gibson, N. P., Aigrain, S., Pont, F., et al. 2012, MNRAS, 422, 753
Hall, J. S. 1949, Sci, 109, 166
Hansen, J. E., & Hovenier, J. W. 1974, JAtS, 31, 1137
Heiles, C. 2000, AJ, 119, 923
Hiltner, W. A. 1949, Natur, 163, 283
Hough, J. H., Lucas, P. W., Bailey, J. A., et al. 2006, PASP, 118, 1302
Huitson, C. M., Sing, D. K., Vidal-Madjar, A., et al. 2012, MNRAS, 422, 2477
Kemp, J. C., & Swedlund, J. B. 1971, Natur, 231, 169
Kemp, J. C., & Wolstencroft, R. D. 1971, Natur, 232, 165
Kopparla, P., Natraj, V., Zhang, X., et al. 2015, ApJ, submitted
Kostogryz, N. M., Yakobchuk, T. M., & Berdyugina, S. V. 2015, ApJ, 806, 97
Kostogryz, N. M., Yakobchuk, T. M., Morozhenko, O. V., & Vid'Machenko, A. P. 2011, MNRAS, 415, 695
Lecavelier Des Etangs, A., Pont, F., Vidal-Madjar, A., & Sing, D. 2008, A&A, 481, L83
Lucas, P. W., Hough, J. H., Bailey, J. A., et al. 2009, MNRAS, 393, 229
Lyot, B. 1929, Ann. Observ. Paris (Meudon), 8, 1
McCullough, P. R., Crouzet, N., Deming, D., & Madhusudhan, N. 2014, ApJ, 791, 55
Michalsky, J. J., & Stokes, R. A. 1974, PASP, 86, 1004
Plaszczynski, S., Montier, L., Levrier, F., & Tristram, M. 2014, MNRAS, 439, 4048
Pont, F., Knutson, H., Gilliland, R. L., Moutou, C., & Charbonneau, D. 2008, MNRAS, 385, 109
Pont, F., Sing, D. K., Gibson, N. P., et al. 2013, MNRAS, 432, 2917
Rages, K., Pollack, J. B., & Smith, P. H. 1983, JGR, 88, 8721
Rice, S. O. 1945, Bell Systems Tech. J., 24, 46
Sing, D. K., Désert, J.-M., Lecavelier Des Etangs, A., et al. 2009, A&A, 505, 891
Sing, D. K., Pont, F., Aigrain, S., et al. 2011, MNRAS, 416, 1443
Tomasko, M. G., Doose, L. R., Dafoe, L. E., & See, C. 2009, Icar, 204, 271
Tomasko, M. G., & Smith, P. H. 1982, Icar, 51, 65
Wardle, J. F. C., & Kronberg, P. P. 1974, ApJ, 194, 249
West, R. A. 1991, ApOpt, 30, 5316
West, R. A., Hart, H., Simmons, K. E., et al. 1983, JGR, 88, 8699
West, R. A., & Smith, P. H. 1991, Icar, 90, 330
Wiktorowicz, S. J. 2009, ApJ, 696, 1116
Wiktorowicz, S. J., & Laughlin, G. P. 2014, ApJ, 795, 12
Wiktorowicz, S. J., & Matthews, K. 2008, PASP, 120, 1282
Wiktorowicz, S. J., Millar-Blanchaer, M., Perrin, M. D., et al. 2014, Proc. SPIE, 9147, 83
Wiktorowicz, S. J., & Nofi, L. A. 2015, ApJL, 800, L1